Pharmaceutical Research, Vol. 26, No. 4, April 2009 (© 2008)
DOI: 10.1007/s11095-008-9778-x

Research Paper

Sonoporation of the Minicircle-VEGF^{165} for Wound Healing of Diabetic Mice

C. S. Yoon,[1] H. S. Jung,[1] M. J. Kwon,[2] S. H. Lee,[2] C. W. Kim,[3] M. K. Kim,[4] M. Lee,[5] and J. H. Park[2,6]

Received August 7, 2008; accepted October 29, 2008; published online November 8, 2008

Purpose. The purpose of this study is to examine the efficiency of sonoporation with minicircle DNA for the skin wound healing in diabetic mice.
Methods. Minicircle DNA containing the human VEGF^{165} was constructed and tested *in vitro*. Diabetes was induced in 2-week old male C57BL/6J mice via streptozotocin (STZ) injection. 6 mm circular skin wounds were made on the mice back. After the subcutaneous injection of the minicircle DNA at the edge of the wound, the mice were exposed to the ultrasound irradiation for the sonoporation. Wound areas were analyzed until the day 12. Blood perfusion and angiogenesis were evaluated using a laser Doppler imaging and CD31 immunostaining, respectively. Re-epithelialization was assessed by histochemical analysis using hematoxylin and eosin staining.
Results. Accelerated wound closure was observed in the mice receiving sonoporation of minicircle-VEGF^{165}, which corresponds to the markedly increased skin blood perfusion and CD31 expression. Histological analysis revealed that the minicircle treated wound tissues showed fully restored normal architectures as compared with the non-treated diabetic controls with the markedly edematous and chaotic morphologies.
Conclusions. Ultrasound mediated gene therapy with the minicircle-VEGF^{165} is effective for the healing of the skin wound of the diabetic mice.

KEY WORDS: diabetic mice; gene delivery; minicircle; sonoporation; wound healing.

INTRODUCTION

Wound healing is an integrative process of complex biological and molecular events. The overlapping phases of wound healing involve coagulation, inflammation, migration–proliferation, and remodeling (1). These processes are characterized by the changes in the composition and organization of the extracellular matrix and the local expression profiles of the various growth factors (2).

VEGF stimulates the formation of the new blood vessels (neo-angiogenesis). EGF, FGF and TGF-α accelerate the formation of the granulation tissue. PDGF primarily acts as a chemo-attractant for the neutrophils and fibroblasts. G-CSF enhances the function of the neutrophils and monocytes. TGF-β is chemotactic for the macrophages and contributes for neo-angiogenesis indirectly and the collagen metabolisms (3).

In diabetic skin ulcers, parts of the wound healing may be blocked in different phases having lost the ideal synchrony of the events required for the normal rapid healing (4,5). The delay of healing is caused by several intrinsic factors from diabetes mellitus itself (hyperglycemia, neuropathy, macro- and micro-angiopathies) and the extrinsic factors (wound infection, callus formation, and excessive pressure to the wound site) (6). Fibroblasts isolated from the diabetic foot ulcers are probably senescent and show a decreased proliferative response to the various growth factors. Macrophages in diabetes show a decrease in the release of various cytokines, including TNF-α, IL-1β, and VEGF (7,8). These intrinsic abnormalities and other extrinsic factors such as hyperglycemia itself and the advanced atherosclerosis compromising the blood supply might contribute to the more complicated wound micro-environment resulting markedly delayed healing (6).

Angiogenesis is a crucial step in the wound healing process by providing a route for oxygen and nutrient delivery, as well as a conduit for the components of the inflammatory response (9,10). That process is regulated by the expressions of a variety of vascular growth factors and modulators (11,12).

Vascular endothelial growth factor (VEGF) is one of the most specific and critical regulators of angiogenesis, which causes increased vascular permeability and deposition of a proangiogenic matrix as well (13). Human VEGF has at least four structurally related isoforms, VEGF^{121}, VEGF^{165}, VEGF^{189}, and VEGF^{206}. VEGF^{165} has the most potent biological activity and is the most abundant subtype *in vivo* (13–15). Delivery of VEGF^{165} by an adeno-associated virus (AAV) vector to the wounds in the rat skins resulted in the

[1] Molecular Therapy Laboratory, Paik Memorial Institute for Clinical Research, Inje University, Busan, South Korea.
[2] Molecular Therapy Laboratory, Paik Memorial Institute for Clinical Research, Paik Diabetes Center, Department of Internal Medicine, Pusan Paik Hospital, College of Medicine, Inje University, 633-165 Gaegum-Dong, Pusanjin-Gu, 614-735, Busan, South Korea.
[3] Department of Pathology, Pusan Paik Hospital, College of Medicine, Inje University, Busan, South Korea.
[4] Department of Internal Medicine, Maryknoll Medical Center, Busan, South Korea.
[5] Department of Bioengineering, Hanyang University, Seoul, South Korea.
[6] To whom correspondence should be addressed. (e-mail: pjhdoc@chol.com)

remarkable induction of the new vessel formation, with consequent reduction of the healing time (16).

Due to the matter of safety and versatility in gene transfer, considerable numbers of studies have been conducted on the non-viral gene carriers. Gene transfer using ultrasound mediated disruption of microbubble is one of these methods, which utilizes the acoustic cavitation of the cell membrane (sonoporation) as the most probable mechanism of transferring drugs or DNA. Jet streams caused by the abrupt explosions of microbubbles adjacent to the cells deliver drugs or DNAs through the cell membrane (17–19). Ultrasound contrast agent, which consists of inert gas-filled microbubbles, is used to promote the ultrasound-mediated transfection (20,21).

Minicircle is a new form of supercoiled DNA molecule for the non-viral gene transfer that has neither bacterial origin of replication nor antibiotic resistance marker. They are thus smaller and potentially safer than the standard plasmids currently used in the non-viral gene therapy. Minicircle DNAs have been demonstrated to show more robust and prolonged transgene expression due to its small size and the absence of un-methylated CpG motifs which causes immune responses (22–24).

Gene transfer of minicircle DNA via sonoporation has never been studied so far. The aim of this study is to assess the efficiency of the gene delivery of minicircle DNA encoding the cDNA of VEGF^{165} by sonoporation to promote the wound healing in streptozotocin (STZ) induced diabetic mice.

MATERIALS AND METHODS

Materials

L-(+)-Arabinose, branched polyethylenimine (BPEI, 25 kDa) and streptozotocin were purchased from Sigma-Aldrich (MO, USA). SonoVue™ was purchased from Bracco (UK). FITC-conjugated anti-CD31 antibody was purchased from Chemicon (CA, USA).

Plasmid Construction

The human VEGF^{165} cDNA was amplified with VEGF-F (5′-CCGAATTCATGAACTTTCTGCTGTCTTGGG-3′), and VEGF-R(5′-AAAAGCGGCCGCTCATTCATTCATCAC-3′) using pSV-VEGF^{165} as a template. Amplification conditions are followed: 2 min at 94°C for initial denaturation, 30 cycles—30 s at 94°C for denaturation, 30 s at 63.4°C for annealing, 1 min at 68°C for extension, 10 min at 72°C for the final extension. All PCRs were carried out in MyCycler™ (Bio-Rad, CA, USA). pβ-VEGF^{165} was constructed by inserting the 595 bp PCR product between the *Eco*RI and *Not*I sites of the empty pβ vector which is driven by the ubiquitous chicken β-actin promoter.

For the production of minicircle DNA, p2øC31-β-VEGF^{165} was constructed. The DNA fragment which only contains the chicken β-actin promoter, VEGF^{165} cDNA and SV40 poly adenylation signal sequence was excised with *Bgl*II and *Cla*I from the pβ-VEGF^{165}, and then bluntly ligated between the attB and attP sites of the p2øC31 plasmid, which was a kind gift from Dr. Mark A. Kay (Department of Genetics, Stanford University, CA, USA).

Preparation of Minicircle-VEGF^{165} DNA

E. coli DH5α (Invitrogen) was transformed by p2øC31-β-VEGF^{165}. A single colony of the transformants was grown at 37°C overnight (OD_{600}=4.5–5.0). The 1 L of bacterial culture in the steady state was spun down in a clinical centrifuge (rotor JA-14, J2-MC centrifuge, Beckman, Fullerton, CA, USA) at 20°C, 1,300×*g* for 15 min. The pellet was re-dissolved with 1 L of fresh LB broth (pH 7.0) containing 1% L-(+)-arabinose. The resuspended bacteria were incubated at 30°C with constant shaking at 225 rpm for 2 h. Subsequently, 1 L of fresh LB broth (pH 9.0) containing 1% L-(+)-arabinose was added to the culture and the bacteria were cultivated for additional 2 h at 37°C for the activation of the restriction enzyme I-SceI. Super-coiled minicircle DNA was prepared from the culture, using plasmid purification kits from the Qiagen (Valencia, CA). The contaminated endotoxin in the DNA preparation was removed by the AffinityPak Detoxi-Gel (Pierce, Rockford, IL).

Cell Culture and Transfection

The human embryonic kidney cells (HEK 293), Chinese hamster ovary cells (CHO) and mouse fibroblast cells (NIH3T3) were purchased from the ATCC (Manassas, VA). HEK293 and NIH3 T3 cells were cultured in DMEM containing 10% fetal bovine serum (FBS) and CHO cells were cultured in F12 medium containing 10% FBS. All cells were maintained in a 5% CO_2 incubator. For the transfection, the cells were seeded at a density of 5.0×10^5 cells/well in the six-well flat-bottomed micro-assay plates (Falcon Co., Becton Dickenson, Franklin Lakes, NJ) 24 h before the transfection. As a gene carrier, BPEI was used. The complexes of DNA and BPEI were prepared at the N/P (molar ratio of BPEI nitrogen to pDNA phosphate) ratio of 10:1 and incubated for 30 min before use. The concentration of BPEI was calculated on the assumption that the molecular weights of a single BPEI unit and a single DNA unit are 43.05 and 330.98 g/mol, respectively. All the cells at 70–80% confluency were transfected with BPEI/DNA polyplexes and incubated for additional 48 h. For the transfection via sonoporation with the microbubble, all cells were detached by trypsin–EDTA, washed twice with the phosphate-buffered saline (PBS), and re-suspended with the serum free media at 2.0×10^5 cells/well in 48-well plate. After addition of the plasmid and the microbubbles, 6.0 mm probe was used for the irradiation of ultrasound with a 20% duty cycle for 30 s (Sonitron 1000, Rich Mar Inc., USA).

For the transfection by equivalent copy number of DNA, the following formula was used:

$$\text{Copy number(molecules/mL)} = \frac{N_A(\text{copies/mol}) \times \text{concentrating(g/mL)}}{N_B \times (330\,\text{Da/base})(\text{g/mol})}$$

(where N_A=Avogadro's number and N_B=number of base).

Cell Viability Measurement

Cell Counting Kit (CCK)-8 assay (Dojindo, Tokyo, Japan) was used for the assessment of the cell viability.

ELISA

The secreted VEGF protein in the media was measured using Quantikine human VEGF ELISA kit (R&D Systems, MN).

Animals

Two-week-old male C57BL/6J mice (20–30 g) were purchased from the Samtako (Animal Breeding Center, Osan, Korea) and housed in the pathogen-free condition and had *ad libitum* access to water and the standard mouse chow. Diabetes mellitus was induced by the single intraperitoneal injection (200 mg kg/wt) of streptozotocin (25). Random blood glucose levels were measured 1 week after the first STZ injection using a glucometer (Accu-Check, Roche Diagnostics). Mice that showed blood glucose levels over 200 mg/dL were considered as diabetic (26).

Skin Wounding

Each animal was subjected to wounding (6 mm in diameter) by punch biopsy (Stiefel, Germany) on the skin of the back of the mouse. Briefly, prior to wounding, general anesthesia was induced by the administration of ketamine hydrochloride (100 mg/kg). The hair was shaved with the standard blade (no. 10) and then, the skin was disinfected with the povidone–iodine solution and wiped with sterile water.

In Vivo Gene Delivery into Diabetic Mouse Wound

Diabetic C57BL/6J mouse with the back skin wound received a subcutaneous injection of PBS containing the mixture of minicircle-VEGF^{165} (20 μg) and microbubble solution (100 μg). Immediately after the injection, ultrasound (frequency, 1.0 MHz, duty, 20%; intensity, 2.0 W/cm^2, time, 30 s) was applied to the injection site of the wound edge using Sonitron 2000 ultrasonicator (Rich-Mar, Inola, OK, USA) with a probe of diameter 6 mm. As controls, the injections of pβ-Null (a control plasmid containing inert gene) and the conventional form of pβ-VEGF^{165} plasmids were performed into the assigned mice with the same protocol.

Measurement of Wound Area and Laser Doppler Imaging (LDI)

The areas of the wounds were evaluated by densitometry (Multi Gauge V3.0 software, Fujifilm Life Science, Tokyo, Japan). Percentage wound closure was calculated as a ratio of final wound area to initial wound area. For the estimation of the skin blood flow, the wounds were scanned with a Laser Doppler Imager (Periscan PIM II Laser Doppler Perfusion Imager, Perimed AB, Sweden) under the brief general anesthesia with inhalation of 1–2% isoflurane on the days 2, 6 and 12. The mice were placed on a light absorbing dark green background. The distance between the scanner head and the object was 20 cm. The Min and Max values were set at 0 and 8 V, respectively. The

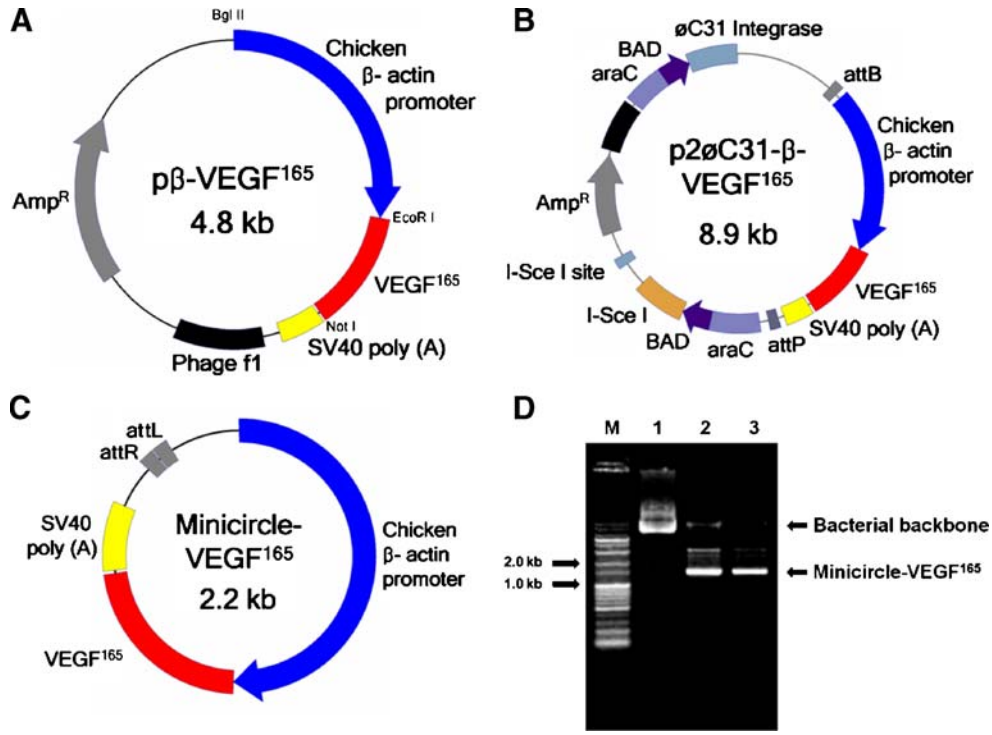

Fig. 1. Physical maps of the constructed vectors. **A** pβ-VEGF^{165}; a conventional plasmid containing bacterially originated backbone. The cDNA sequence coding VEGF^{165} was inserted under a chicken β-actin promoter. **B** p2øC31-β-VEGF^{165}; the expression cassette from pβ-VEGF^{165} was excised by restriction enzymes and bluntly ligated between attB and attP site of p2øC31 vector which contains phi-C31 integrase and I-SceI homing endonuclease. **C** Minicircle-VEGF^{165}. **D** Process of minicircle-VEGF^{165} production. By adding 1%-L-arabinose to the bacterial culture media, the att sites of p2øC31-β-VEGF^{165} (*lane 1*) were recombined to generate the minicircle DNA (*lane 2*). The remaining circular bacterial backbone plasmids were linearized by I-SceI homing endonuclease and were removed by bacterial exonucleases at 37°C (*lane 3*).

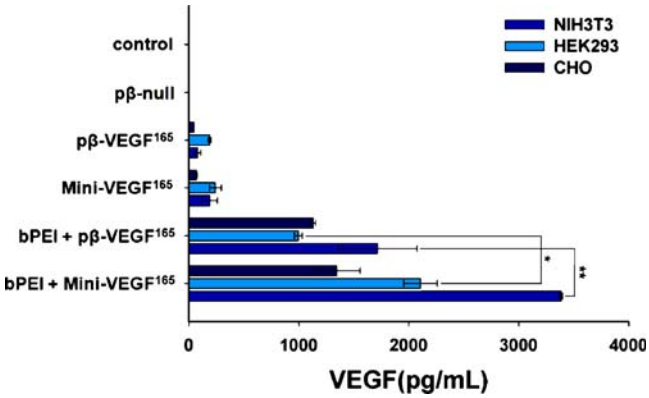

Fig. 2. Minicircle-VEGF^{165} showed enhanced transfection efficiency in the various cell lines. 2×10^5 cells of CHO, HEK293 and NIH3T3 were treated for 4 h with plasmid DNA (pβ-VEGF^{165} or Minicircle-VEGF^{165}) complexed with or without branched polyethylenimine (25 kDa, N/P ratio 10:1). VEGF concentrations in the culture media were measured by ELISA. In HEK293 and NIH3T3 cells, up to 2.5 fold higher gene expressions by minicircle-VEGF^{165} DNA were observed than the conventional plasmid, pβ-VEGF^{165} (*$p<0.05$). All used plasmids were diluted to have equal copy number (3.75×10^{17}copies per μg).

perfusion scan image color scale displayed the lowest value in dark blue and the highest value in red, which represent the relative amount of skin blood perfusion. All mice were placed on a warming pad to maintain core body temperature between 36.8°C and 37.8°C during the scanning.

Immunohistochemistry

The tissue samples adjacent to the wounds were embedded in OCT compound (Tissue Tek, Sakura Finetek USA). Transverse sections of 5 μm thickness were placed onto poly-l-lysine-coated slides. CD31 was detected with FITC-conjugated anti-CD31 antibody (1:100) and observed under a green fluorescence microscope, Olympus BX-51 (Olympus, Tokyo, Japan). Image J software (http://rsb.info.nih.gov/ij/) was used to quantify CD31 positive area.

Histology

On the day 12, wound tissues were fixed in 4% phosphate buffered formalin and then embedded in paraffin. From the paraffin-embedded tissue blocks, 5 μm sections were cut and stained with hematoxylin–eosin (HE) for the histological analysis.

Statistical Analysis

All the presented data were expressed as mean±SD, and the statistical significance were analyzed by the Student's *t*-test and ANOVA using the SPSS PC program.

RESULTS

We constructed the minicircle-VEGF^{165} DNA (Fig. 1) free from the un-methylated CpG motifs present in bacterial DNA which might cause immune responses in the mammalian system. The human VEGF^{165} cDNA was successfully cloned by PCR and ligated into the plasmid pβ driven by the ubiquitous chicken β-actin promoter resulting in plasmid pβ-VEGF^{165}. Chicken β-actin promoter was reported to exhibit high levels of reporter gene expression and the relatively low levels of T cell trans-activation (27).

From pβ-VEGF^{165}, the expression cassette which only contains the promoter, the VEGF^{165} gene, and the poly adenylation sequence was excised by restriction enzyme digestion with *Bgl*II and *Cla*I, and ligated between the attB and attP sites of the plasmid p2øC31. At 30°C, by addition of arabinose, *phage* øC31 integrase and *Saccharomyces cerevisiae* homing endonuclease I-SceI were induced. The øC31 integrase performed a site-specific recombination of sequences between attB and attP recognition sites, splitting p2øC31-VEGF^{165} into two super-coiled circular DNAs; the minicircle-VEGF^{165} and the remaining DNA with bacterial backbone. By adjusting the pH and the temperature to pH 9.0 and 37°C, respectively, the accompanying bacterial DNA was linearized by the induced I-SceI and degraded by bacterial exonucleases (Fig. 1D). As a consequence, only the minicircle-VEGF^{165} (2,204 bp) remained intact in the form of episome in bacterial cytosol.

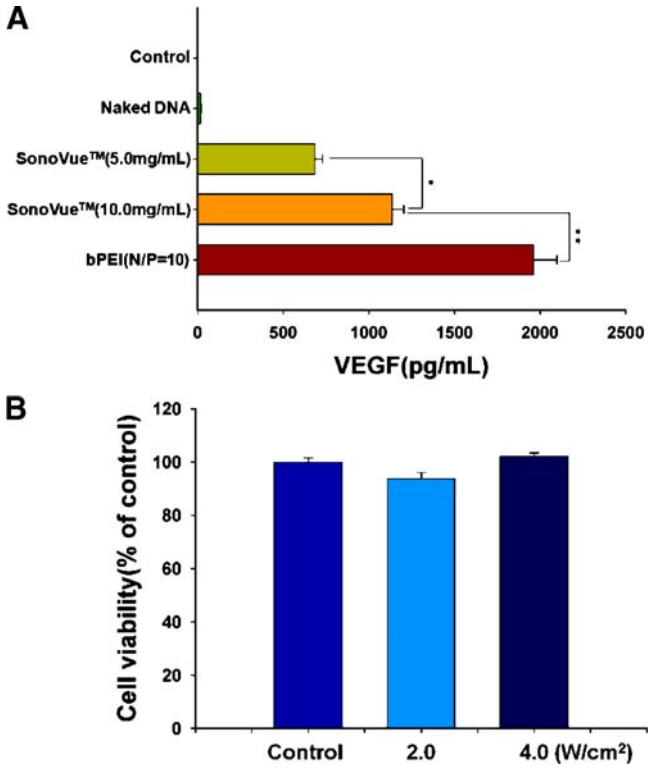

Fig. 3. The effects of sonoporation on the transfection efficiency and the cell viability. **A** HEK293 cells were transfected with 2 μg of pβ-VEGF^{165} by 1-MHz ultrasound with varying concentrations of microbubbles (exposure intensity, 2 W/cm^2; duty cycle, 20% for 30 s). In our experiment, the VEGF expression by sonoporation with 10 mg/mL SonoVue™ microbubbles was about the half of that by branched polyethylenimine (25 kDa) at the N/P ratio of 10:1 ($p<0.05$). **B** The viability of HEK293 cells for the various intensities of ultrasound. The ultrasound exposure intensity up to 4.0 W/cm^2 (1-MHz ultrasound; duty cycle, 20% for 30 s) demonstrated no apparent effect on the cell viability. The cell viability was measured by CCK-8. *Error bars* are the SE of the mean cell viability obtained from the three independent experiments ($p<0.05$).

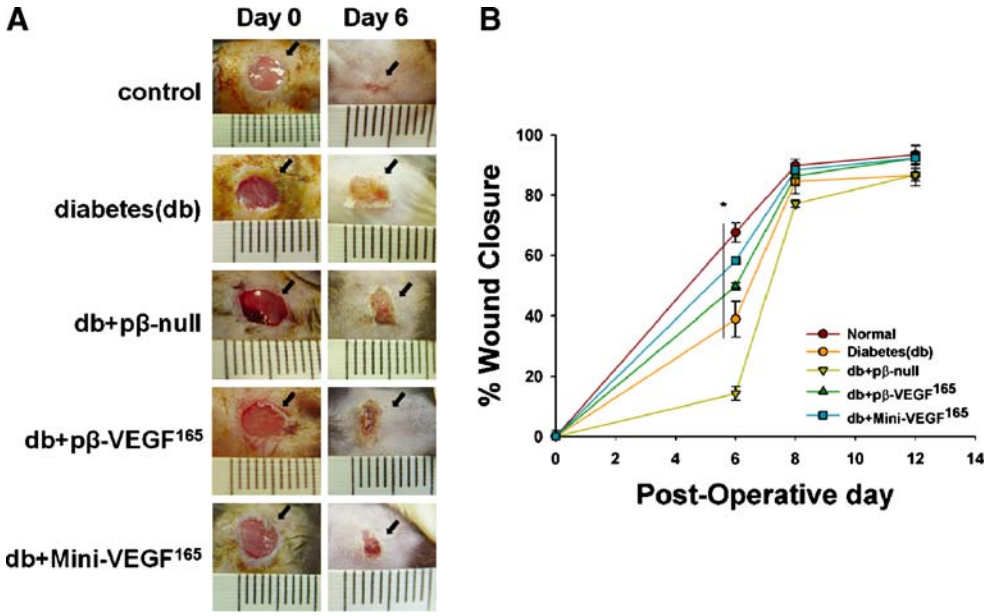

Fig. 4. Minicircle-VEGF^{165} gene delivery via sonoporation enhanced wound closure. **A** Macroscopic pictures of the wounds. **B** Average area (in pixels) of the wounds of the minicircle-VEGF^{165} treated diabetic mice was significantly small as compared with those of diabetic control and pβ-VEGF^{165} treated diabetic mice. Minicircle-VEGF^{165} treatment promoted diabetic wound closure (*$p<0.05$).

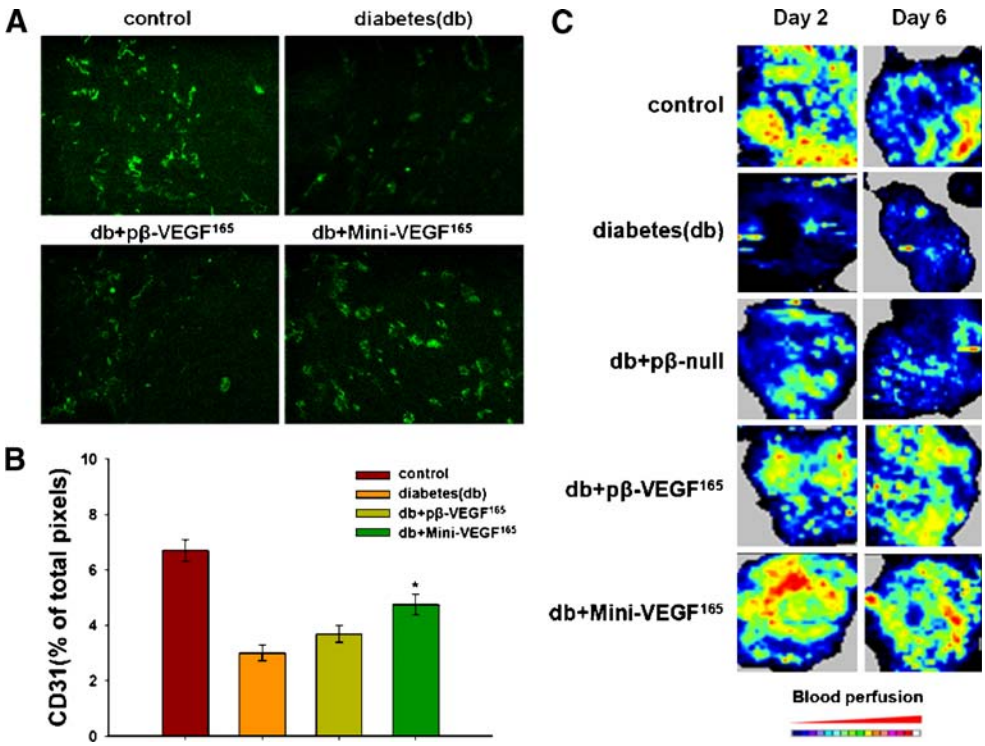

Fig. 5. Minicircle-VEGF^{165} increased capillary density and blood perfusion in the wound tissue of treated diabetic mice. **A** Immunohistochemistry. In the plasmid DNA treated group, the density of microvessels was markedly increased in the minicircle-VEGF treated diabetic wound ($p<0.05$). **B** LDI of wound tissues treated with pβ-Null (inert gene), pβ-VEGF^{165} and minicircle-VEGF^{165}. Significantly increased blood perfusion was observed in the wound tissues treated with minicircle-VEGF^{165} up to the 6 day after treatment.

To assess the transfection efficiency of the minicircle-VEGF^{165}, the expression level of VEGF was evaluated by ELISA. To determine the optimum N/P ratio for BPEI as a gene carrier, we performed gel retardation assay for the completeness of complexation, and repeatedly performed *in-vitro* transfection with varying N/P ratios between 0 and 20. We finally decided to use N/P ratio 10:1 in our comparative *in-vitro* experiment. According to our results and the previous literature, usually the N/P ratio 10:1 is the optimum condition when using BPEI, because of the maximum transfection efficiency with the appreciable cytotoxicity (28).

Minicircle-VEGF^{165} showed 2.5-fold higher transgene expression than the equivalent copy numbers of conventional plasmid (pβ-VEGF^{165}) in HEK293 and NIH3T3 cells (Fig. 2). In CHO cells, the total transgene expression levels were not high as compared with the other cell lines. This difference might be regarded as cell-line dependent. As a whole, minicircle-VEGF^{165} maintained higher transfection efficiency than the conventional counterparts in the various cell lines using BPEI (N/P ratio 10:1) as a carrier.

Although BPEI has been reported as one of the most effective non-viral gene carrier, the potential cytotoxicity limits its wide-spread clinical applications (29). The transfection efficiency of the sonoporation depends on the various factors such as ultrasound intensity, duration cycle, and especially the concentration of microbubbling agent (30). In our study, sonoporation of pβ-VEGF^{165} with microbubble (10 mg/mL) showed about half of transgene expression as compared with the BPEI mediated gene delivery (N/P ratio of 10) in HEK293 cells (Fig. 3A). 1-Mhz ultrasound with exposure intensity up to 4 W/cm^2 did not affect the viability of the cells (Fig. 3B).

We analyzed the effect on wound healing by VEGF^{165} sonoporation gene therapy in the STZ-diabetic C57BL/6J mice (n=15). STZ-diabetic mice model has been widely used in the various kinds of diabetes complications experiments, including the impaired wound healing researches (31,32). STZ induces diabetes mellitus via the complete destruction of insulin secreting pancreatic β-cells (33).

Normal mice showed blood glucose levels of 102±10 mg/dL (n=5). 1 week after a single high dose of intra-peritoneal STZ injection (200 mg kg·wt^{-1}), blood glucose levels increased to remain elevated over 400±10 mg/dL throughout the entire experimental period. In the high blood glucose level, the wound tissue showed decreased growth factor levels (VEGF, EGF, TGF-β and PDGF) via Western blot analyses which is concurrent with the impaired wound healing of diabetes (data not shown) (34,35).

The results for the changes of the percentages of wound closure in control and diabetic mice are shown in Fig. 4. By the day 12, all normal controls and VEGF^{165} treated groups demonstrated complete closure of the wounds in contrast to diabetic control with a mean percent closure below 80%. The differences among the groups were statistically significant at the day 6 (p<0.05). The mean percent wound closure of the minicircle-VEGF^{165} treated mice was 58.2%, which is significantly better than the diabetic controls (38.1%). The conventional pβ-VEGF^{165} injection demonstrated 49.0%, while pβ-null plasmid treated mice showed only 14.2%.

The wound tissue samples from the each experimental group at the day 2 were stained with the FITC-conjugated anti-CD31 antibody (Fig. 5). CD31 positivity reflects the degree of neo-angiogenesis. The results indicate that the CD31-positive area was significantly decreased in the diabetic control as compared with the normal control group. We found that the CD31 expression was significantly increased in the minicircle-VEGF^{165} treated mice (Fig. 5B), which corresponds well to the results of the skin blood perfusion measured by LDI at the day 2 (Fig. 5C). The differences of wound blood perfusion were monitored by LDI at the day 2 and 6 (Fig. 5C). In comparison with the normal control, diabetic control demonstrated significantly decreased blood perfusion. The minicircle-VEGF^{165} DNA treated diabetic mice showed significantly increased blood flow in the wound area. Skin blood perfusions were gradually decreased after the day 12 (data not shown).

The histology of biopsied wound tissues at the day 12 are shown in Fig. 6. The wound of diabetic control shows severe edema and disorganized pattern with the heavy infiltration of the inflammatory cells. Sonoporation gene therapy using minicircle VEGF^{165} nearly completely restored wound microarchitectures into normal.

DISCUSSION

In our study, we could not demonstrate whether the total required time for the complete wound closure was shortened by VEGF gene therapy. Because of the small initial size of the

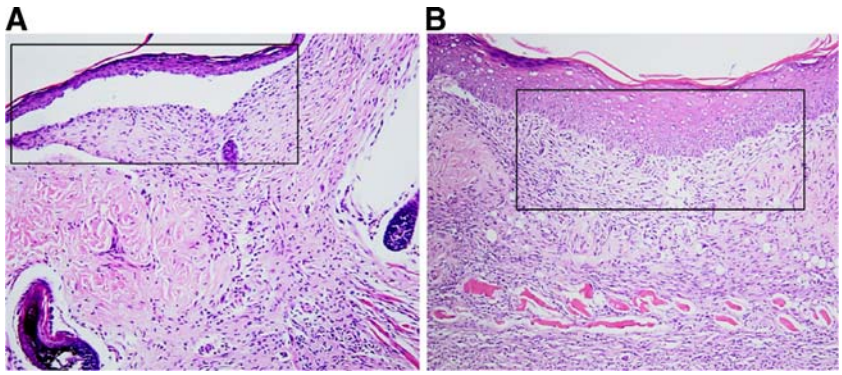

Fig. 6. Histologies of the healing wound tissues at the day 12. **A** Diabetic wound shows severe edema, disorganized microarchitectures and the heavy infiltration of the inflammatory cells. **B** The wound of diabetic mouse with minicircle-VEGF^{165} DNA sonoporation shows nearly complete restoration of microarchitectures into normal.

wounds, progressive contracture of the wound margin and scar formation made it very difficult to compare. If the initial wound size is large enough seen in the clinical practice, we believe that the total required time for the wound closure might be shortened via VEGF gene therapy. The histological improvement with VEGF gene therapy at day 12 in contrast to the chaotic microarchitecture of the diabetic control might mean that the healing process in diabetic animal was clearly abnormal despite of the gross closure of the wounds. Complete healing process including the remodeling requires over 3 months, and the incomplete histological healing in the diabetics might predispose the recurrence.

Concerning the matter of safety, non-viral gene therapy in the wound healing has several advantages over the viral gene therapy. Most methods are simple, inexpensive and have no additional risk of inflammation and infection. The timed gene expression should be regarded as an advantage in the wound healing where stable life-long expression is not required.

An ideal gene delivery system would enhance gene expression in the target while having no effect in non-target tissues. Sonoporation with microbubble might be able to make it possible to localize gene delivery. Ultrasound has been shown to enhance gene transfer into cells *in vitro* and *in vivo*. Sonoporation to different tissues has been reported, including solid tumors, muscle and vasculature (36–39). Enhanced gene transfer is found either when the exposed bubbles are in the vicinity of the genetic material, or when the genes are encapsulated within, or bound to the bubbles. The micro-bubbling agent SonoVue™, a second-generation ultrasound contrast agent, is composed of sulfur hexafluoride gas stabilized by a highly flexible phospholipid shell. SonoVue™ has been well tolerated and has been safely administered to over 1,800 human subjects in the previous clinical trials (40).

Our study showed that the non-viral gene therapy using minicircle-VEGF^{165} DNA exhibited two to three folds higher gene expression than the conventional plasmid *in vitro* and exhibited more improved biological safety characteristics. This could be due to either the removal of the unnecessary plasmid sequences, which could affect the gene expression or the smaller size of the minicircle plasmid which might confer better extracellular and intracellular bioavailability and result in improved gene delivery properties (22–24). Particularly, this increased and long-lasting transgene expression of minicircle DNA might compensate for the relatively low efficiency of non-viral gene delivery methods.

In conclusion, our results demonstrated that the non-viral gene therapy with minicircle DNA encoding VEGF^{165} via sonoporation could improve the healing of skin wounds in STZ-induced diabetic mice, which might be applied in the actual human clinical trial in the near future.

ACKNOWLEDGEMENTS

The part of this work was accepted as an abstract at the 42nd Annual Meeting of the European Association for the Study of Diabetes in Denmark Copenhagen-Malmoe, September 2006. The present study was financially supported by the Inje University Research Grant 2005. We thank Dr. Mark A Kay (Stanford University) for generously providing plasmid p2øC31.

REFERENCES

1. P. Martin. Wound healing—aiming for perfect skin regeneration. *Science*. **276**:75–81 (1997) doi:10.1126/science.276.5309.75.
2. A. J. Singer, and R. A. Clark. Cutaneous wound healing. *N. Engl. J. Med.* **341**:738–746 (1999) doi:10.1056/NEJM199909023411006.
3. S. Enoch, and D.J. Leaper. Basic science of wound healing. *Surgery(Oxford)*. **26**:31–37 (2008) doi:10.1016/j.mpsur.2007.11.005.
4. M. A. Loot, S. B. Kenter, F. L. Au, W. J. van Galen, E. Middelkoop, J. D. Bos, and J. R. Mekkes. Fibroblasts derived from chronic diabetic ulcers differ in their response to stimulation with EGF, IGF-I, bFGF and PDGF-AB compared to controls. *Eur. J. Cell Biol.* **81**:153–160 (2002) doi:10.1078/0171-9335-00228.
5. M. A. Loots, E. N. Lamme, J. Zeegelaar, J. R. Mekkes, J. D. Bos, and E. Middelkoop. Differences in cellular infiltrate and extracellular matrix of chronic diabetic and venous ulcers *versus* acute wounds. *J. Invest. Dermatol.* **111**:850–857 (1998) doi:10.1046/j.1523-1747.1998.00381.x.
6. W. J. Jeffcoate, and K. G. Harding. Diabetic foot ulcers. *Lancet*. **361**:1545–1551 (2003) doi:10.1016/S0140-6736(03)13169-8.
7. T. Dinh, and A. Veves. Microcirculation of the diabetic foot. *Curr. Pharm. Des.* **11**:2301–9 (2005) doi:10.2174/1381612054367328.
8. Y. Tsurumi, S. Takeshita, D. Chen, M. Kearney, S. T. Rossow, J. Passeri, J. R. Horowitz, J. F. Symes, and J. M. Isner. Direct intramuscular gene transfer of naked DNA encoding vascular endothelial growth factor augments collateral development and tissue perfusion. *Circulation*. **94**:3281–3290 (1996).
9. J. Folkman. Angiogenesis in cancer, vascular, rheumatoid and other disease. *Nat. Med.* **1**:27–31 (1995) doi:10.1038/nm0195-27.
10. V. Falanga. The chronic wound: impaired healing and solutions in the context of wound bed preparation. *Blood Cells Mol. Diseases*. **32**:88–94 (2004) doi:10.1016/j.bcmd.2003.09.020.
11. J. Plouet, J. Schilling, and D. Gospodarowicz. Isolation and characterization of a newly identified endothelial cell mitogen produced by AtT-20 cells. *EMBO J.* **8**:3801–3806 (1989).
12. N. Ferrara, and W. J. Henzel. Pituitary follicular cells secrete a novel heparin-binding growth factor specific for vascular endothelial cells. *Biochem. Biophys. Res. Commun.* **161**:851–858 (1989) doi:10.1016/0006-291X(89)92678-8.
13. T. Alon, I. Hemo, A. Itin, J. Pe'er, J. Stone, and E. Keshet. Vascular endothelial growth factor acts as a survival factor for newly formed retinal vessels and has implications for retinopathy of prematurity. *Nat. Med.* **1**:1024–1028 (1995) doi:10.1038/nm1095-1024.
14. F. Yuan, Y. Chen, M. Dellian, N. Safabakhsh, N. Ferrara, and R. K. Jain. Time-dependent vascular regression and permeability changes in established human tumor xenografts induced by an anti-vascular endothelial growth factor/vascular permeability factor antibody. *Proc. Natl. Acad. Sci. U. S. A.* **93**:14765–14770 (1996) doi:10.1073/pnas.93.25.14765.
15. K. A. Houck, N. Ferrara, J. Winer, G. Cachianes, B. Li, and D. W. Leung. The vascular endothelial growth factor family: identification of a fourth molecular species and characterization of alternative splicing of RNA. *Mol. Endocrinol.* **5**:1806–1814 (1991).
16. B. Deodato, N. Arsic, L. Zentilin, M. Galeano, D. Santoro, V. Torre, D. Altavilla, D. Valdembri, F. Bussolino, F. Squadrito, and M. Giacca. Recombinant AAV vector encoding human VEGF165 enhances wound healing. *Gene Ther.* **9**:777–785 (2002) doi:10.1038/sj.gt.3301697.
17. H. J. Kim, J. F. Greenleaf, R. R. Kinnick, J. T. Bronk, and M. E. Bolander. Ultrasound-mediated transfection of mammalian cells. *Hum. Gene Ther.* **7**:1339–1346 (1996) doi:10.1089/hum.1996.7.11-1339.
18. D. B. Tata, F. Dunn, and D. J. Tindall. Selective clinical ultrasound signals mediate differential gene transfer and expression in two human prostate cancer cell lines: LnCap and PC-3. *Biochem. Biophys. Res. Commun.* **234**:64–67 (1997) doi:10.1006/bbrc.1997.6578.
19. S. Bao, B. D. Thrall, and D. L. Miller. Transfection of a reporter plasmid into cultured cells by sonoporation *in vitro*. *Ultrasound Med. Biol.* **23**:953–959 (1997) doi:10.1016/S0301-5629(97)00025-2.
20. P. A. Grayburn. Current and future contrast agents. *Echocardiography*. **19**:259–265 (2002) doi:10.1046/j.1540-8175.2002.00259.x.

21. M. W. Miller. Gene transfection and drug delivery. *Ultrasound Med. Biol.* **26**(Suppl 1):S59–S62 (2000) doi:10.1016/S0301-5629(00)00166-6.
22. A. M. Darquet, B. Cameron, P. Wils, D. Scherman, and J. Crouzet. A new DNA vehicle for nonviral gene delivery: supercoiled minicircle. *Gene Ther.* **4**:1341–1349 (1997) doi:10.1038/sj.gt.3300540.
23. A. M. Darquet, R. Rangara, P. Kreiss, B. Schwartz, S. Naimi, P. Delaere, J. Crouzet, and D. Scherman. Minicircle: an improved DNA molecule for *in vitro* and *in vivo* gene transfer. *Gene Ther.* **6**:209–218 (1999) doi:10.1038/sj.gt.3300816.
24. Z. Y. Chen, C. Y. He, A. Ehrhardt, and M. A. Kay. Minicircle DNA vectors devoid of bacterial DNA result in persistent and high-level transgene expression *in vivo*. *Mol. Ther.* **8**:495–500 (2003) doi:10.1016/S1525-0016(03)00168-0.
25. K. Ramabadran, M. Bansinath, H. Turndorf, and M. M. Puig. The hyperalgesic effect of naloxone is attenuated in streptozotocin-diabetic mice. *Psychopharmacology (Berl)*. **97**:169–174 (1989) doi:10.1007/BF00442244.
26. M. Anjaneyulu, and P. Ramarao. Studies on gastrointestinal tract functional changes in diabetic animals. *Methods Find. Exp. Clin. Pharmacol.* **24**:71–75 (2002) doi:10.1358/mf.2002.24.2.677129.
27. E. L. Weber, and P. M. Cannon. Promoter choice for retroviral vectors: transcriptional strength *versus* trans-activation potential. *Hum. Gene Ther.* **18**:849–860 (2007) doi:10.1089/hum.2007.067.
28. H. Hee. Ahn, M. S. Lee, M. H. Cho, Y. N. Shin, J. H. Lee, K. S. Kim, M. S. Kim, G. Khang, K. C. Hwang, I. W. Lee, S. L. Diamonde, and H. B. Lee. DNA/PEI nano-particles for gene delivery of rat bone marrow stem cells. *Colloids Surf. A, Physicochem. Eng. Asp.* **328**:1–7 (2008) doi:10.1016/j.colsurfa.2008.06.011.
29. H. Lv, S. Zhang, B. Wang, S. Cui, and J. Yan. Toxicity of cationic lipids and cationic polymers in gene delivery. *J. Control. Release.* **114**:100–9 (2006) doi:10.1016/j.jconrel.2006.04.014.
30. S. Mehier-Humbert, and R. H. Guy. Physical methods for gene transfer: improving the kinetics of gene delivery into cells. *Adv. Drug Deliv. Rev.* **57**:733–53 (2005) doi:10.1016/j.addr.2004.12.007.
31. E. Seifter, G. Rettura, J. Padawer, F. Stratford, D. Kambosos, and S. M. Levenson. Impaired wound healing in streptozotocin diabetes. Prevention by supplemental vitamin A. *Ann. Surg.* **194**:42–50 (1981) doi:10.1097/00000658-198107000-00008.
32. R. Tsuboi, C. M. Shi, D. B. Rifkin, and H. Ogawa. A wound healing model using healing-impaired diabetic mice. *J. Dermatol.* **19**(11):673–675 (1992).
33. W. J. Schnedl, S. Ferber, J. H. Johnson, and C. B. Newgard. STZ transport and cytotoxicity. Specific enhancement in GLUT2-expressing cells. *Diabetes*. **43**:1326–1333 (1994) doi:10.2337/diabetes.43.11.1326.
34. G. Lauer, S. Sollberg, M. Cole, I. Flamme, J. Sturzebecher, K. Mann, T. Krieg, and S. A. Eming. Expression and proteolysis of vascular endothelial growth factor is increased in chronic wounds. *J. Invest. Dermatol.* **115**:12–18 (2000) doi:10.1046/j.1523-1747.2000.00036.x.
35. B. A. Mast, and G. S. Schultz. Interactions of cytokines, growth factors, and proteases in acute and chronic wounds. *Wound Repair Regen.* **4**:411–420 (1996) doi:10.1046/j.1524-475X.1996.40404.x.
36. Y. Taniyama, K. Tachibana, K. Hiraoka, M. Aoki, S. Yamamoto, K. Matsumoto, T. Nakamura, T. Ogihara, Y. Kaneda, and R. Morishita. Development of safe and efficient novel nonviral gene transfer using ultrasound: enhancement of transfection efficiency of naked plasmid DNA in skeletal muscle. *Gene Ther.* **9**:372–80 (2002) doi:10.1038/sj.gt.3301678.
37. Q. L. Lu, H. D. Liang, T. Partridge, and M. J. Blomley. Microbubble ultrasound improves the efficiency of gene transduction in skeletal muscle *in vivo* with reduced tissue damage. *Gene Ther.* **10**:396–405 (2003) doi:10.1038/sj.gt.3301913.
38. Y. Taniyama, K. Tachibana, K. Hiraoka, T. Namba, K. Yamasaki, N. Hashiya, M. Aoki, T. Ogihara, K. Yasufumi, and R. Morishita. Local delivery of plasmid DNA into rat carotid artery using ultrasound. *Circulation*. **105**:1233–1239 (2002) doi:10.1161/hc1002.105228.
39. P. E. Huber, M. J. Mann, L. G. Melo, A. Ehsan, D. Kong, L. Zhang, M. Rezvani, P. Peschke, F. Jolesz, V. J. Dzau, and K. Hynynen. Focused ultrasound (HIFU) induces localized enhancement of reporter gene expression in rabbit carotid artery. *Gene Ther.* **10**:1600–1607 (2003) doi:10.1038/sj.gt.3302045.
40. S. Mayer, and P. A. Grayburn. Myocardial contrast agents: recent advances and future directions. *Prog. Cardiovasc. Dis.* **44**:33–44 (2001) doi:10.1053/pcad.2001.26438.